Int. J. Electrochem. Sci., 16 **(2021)** Article ID: 210756, doi: 10.20964/2021.07.51

International Journal of
ELECTROCHEMICAL
SCIENCE
www.electrochemsci.org

Preparation of Vapor Grown Carbon Fiber/2-((4-dimethylamino) phenyl) amino) naphthalene-1, 4-dione Composites and their supercapacitor properties

Latifatu Mohammed[1,], Hu Mengyang[2], Hamenu Louis[3], Alfred Madzvamuse[4], Andrew Nyamful[5], David Dodoo-Arhin[6], Andrews Danquah[7], Odoi King Manteaw[8], Mohammed Nafiu Zainudeen[5], Samuel Agyekum Darkwa[5] Jeong Ho Park[2], Jang Myoun Ko[2]*

[1] Division of Sustainable Energy Technologies, Council for Scientific and Industrial Research-Institute of Industrial Research, P. O. Box LG 587, Ghana
[2] Department of Applied Chemistry & Biotechnology, Hanbat National University, 125 Dongseo-daero, Deokmyeong-dong, Yuseong-gu, Daejeon, South Korea.
[3] Department of Chemistry, School of Physical and Mathematical Sciences, College of Basic and Applied Sciences University of Ghana, Legon, Ghana.
[4] Department of Chemistry, University of Zimbabwe, P. O. MP 167, Mount Pleasant, Harare, Zimbabwe
[5] Department of Nuclear Engineering, Graduate School of Nuclear and Allied Sciences, University of Ghana, Ghana
[6] Department of Materials Science & Engineering, University of Ghana, Annie Jiaggie Road, Legon-Accra, Ghana.
[7] Department of Molecular Biology and Biotechnology, University of Cape Coast, Cape coast
[8] Biotechnology and Nuclear Agricultural Research Institute, Ghana Atomic Energy Commission, Ghana
[*]E-mail: latifatu.mohammed@yahoo.com

Received: 11 February 2021 / *Accepted:* 9 April 2021 / *Published:* 31 May 2021

In this work, a derivative of 1,4-dihydoxynaphthalene, 2-((4-dimethylamino) phenyl) amino) naphthalene-1,4-dione (HBU) was synthesized by reacting 1,4-dihydoxynaphthalene with N, N-Dimethyl-p-phenylenediamine. The supercapacitive properties of the electrodes containing various weights percent of vapor grown carbon fiber (VGCF) and HBU were probed in terms of redox behavior, the effect of VGCF, and specific capacitance. The VGCF created an excellent electronic pathway in the electrode, boosting the redox transition reaction in HBU involving a total of three-electron ($3e^-$)-three-proton ($3H^+$) processes corresponding to 2,3-dihydro1,4-naphthoquinone–1,4-dihydroxynaphthalene and the aliphatic amine in the backbone of the substituted derivative of aniline. This led to a higher specific capacitance of 98 F/g for the HBU-VGCF electrode with a higher weight percent of HBU. The capacity retention of about 57% was observed for the HBU-VGCF electrodes after the 1000^{th} cycle owing to the VGCF supporting the HBU by stabilizing its redox activity.

Keywords: vapor grown carbon fiber, 1, 4-dihydoxynaphthalene, electrode, supercapacitor

1. INTRODUCTION

Supercapacitors (SC), also referred to as ultracapacitors, are energy-storing gadgets with high performance, low internal resistance and the capacity to offer high power compared to batteries. Based on their charge storage mechanism, supercapacitors can be classified as either electric double layer capacitor, for which there is no transfer of an electron between the electrodes and the charges are stored electrostatically (non-faradaic), or a pseudocapacitor, an electron transfer process that stores charges faradaically [1, 2]. A SC consists of two electrodes, a separator, and an electrolyte [3, 4]. Compared to other energy-storing gadgets, a SC has its own advantages, such as being lightweight and low maintenance; having a long cycle life, flexible packaging and high power; and enduring a range of temperatures [5]. SCs can best be applied in areas such as computers, light emission hybrid cars/buses, temporary energy storage gadgets when used simultaneously with batteries, etc. [6, 7]. A number of materials have been investigated as supercapacitor electrodes [8]. Oxides of some metal [9] have demonstrated qualities of the best SC electrode material, contributing to great capacitance, but cost and accessibility have hindered their commercial application. Intrinsically conducting polymers, mostly organic in nature, have also gained recognition. They offer a constant range of oxidation states, thus resulting in an increase in the electric voltage of the electrode [10, 11], but their stability is a considerable challenge for researchers.

Quinones and their derivatives have received considerable interest as materials for electrodes in energy storage gadgets such as lithium-ion batteries [12, 13], redox flow batteries [14], electrochemical capacitors [15] and polymer/air batteries [16, 17]. Quinones and their derivatives are promising organic raw materials for electrochemical cells because they are economical, environmentally harmless and demonstrate high cycle reversibility [18]. They are a group of redox-active organic complexes that contain two adjacent carbonyl groups in an unsaturated six-membered ring arrangement [19, 20]. The redox activity of quinones plays a significant role in the electrochemical response during the biological energy transfer of genetic materials and energy storage gadgets. Additionally, the reduced forms of quinone are obtained by accepting protons and electrons, a process which contributes to long-lasting charge separation with little charge reintegration. The behavior of quinones and their derivatives with regard to their electron transfer and proton couple mechanism has motivated researchers to upgrade the effectiveness of supercapacitors, solar cells, batteries, artificial photosynthesis, biofuel cells, and photochemical water separation gadgets [21–27]. The theoretical capacitance of quinone-based compounds has been discovered to be high or comparable to lithium ion batteries [28]. On the other hand, the development of quinone based materials as electrodes for energy storage devices over the years has encountered drawbacks such as low redox kinetics [29], excessive solubility in organic electrolytes [28] and insufficient electrical conductivity. These drawbacks have resulted in low capacitance compared to their theoretical capacitance [30, 31]. Recent studies have shown the utilization of quinones and their derivatives in energy storage gadgets through the amalgamation of quinone molecules and different inorganic and organic materials [32-36]. The easiest means to enhance the electrical trait of materials is to modify the material by putting in electrically conductive substances to create a composite. Much work has gone into modifying the properties of quinone and its derivatives by adding conductive carbon materials. Some of these studies have dealt with the decorating of quinones with highly conductive carbon materials such as carbon nanotubes/fibers, carbon onions, graphite, graphene, and carbon black for stable performance and high capacitance [37-42]. Fiber-based conductive carbon material has been utilized in

electrochemical cells as a support [43] or as a conductive additive [44] for electrode materials, as a result of their special thermal stability, good mechanical property, good corrosion resistance and electrochemical stability in various electrolyte solutions [45].

Blending faradaic pseudocapacitive material with electrical conducting materials (fiber) could help enhance their electrical conductivity, reversibility and charge storage capacity through the establishing of an efficient electron carriage network [46]. Among fiber based carbon materials, vapor-grown carbon fiber (VGCF) is obtained by the break-down of hydrocarbons in the presence of a metal catalyst at elevated temperatures [47]. These fibers are found to induce superior properties in electrodes of electrochemical devices as a result of their high surface to volume ratio and electron conductivity [48, 49]. In this study, a 1, 4-dihydroxynaphthalene derivative compound, 2-((4-dimethylamino) phenyl) amino) naphthalene-1, 4-dione (HBU) was synthesized chemically. The effect of VGCF on the capacity enhancement and the electrochemical properties of the synthesized particles as a supercapacitor electrode was investigated.

2. EXPERIMENTAL

2.1. Synthesis and characterization of HBU

(100mg, 1.0eq) of 1,4-Dihydroxynaphthalene was dissolved in EtOH. (23mg, 0.1eq) of $CeCl_3.H_2O$ and (101.9mg, 1.2eq) of N, N-Dimethyl- p-phenylenediamine was added under continuous stirring. (0.26ml, 3.0eq) of Triethylamine was added drop wise and the mixture was stirred at ambient temperature for 24 hrs. The synthetic route is shown in Fig. 1a.

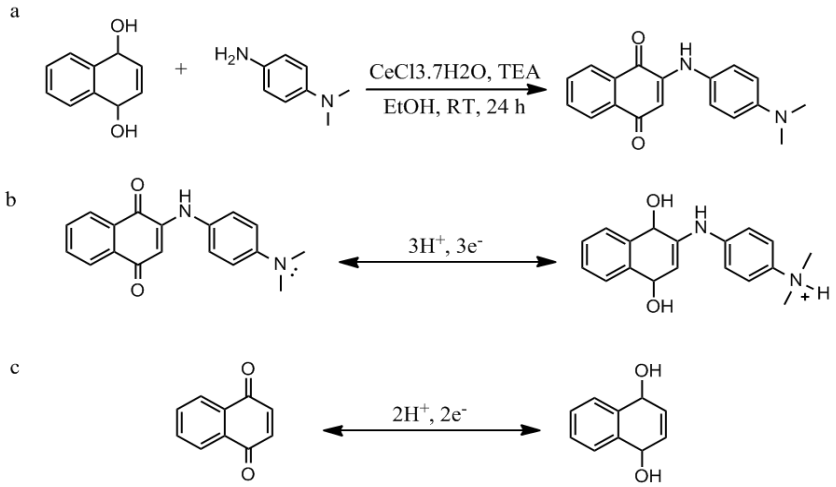

Figure 1. (a) Synthesis reaction of the HBU from 1, 4-dihydoxynaphthalene and N, N-Dimethyl- p-phenylenediamine; (b) redox reaction of the HBU (c) Chemical reaction of PhQ-$PhQH_2$ transitions

The completion of the reaction was confirmed with chromatography using a solvent mixture of 1:1 ethyl acetate: hexane. Water was used to crystalize the final product, which was then filtered and finally dried at 100 ^oC with a reaction yield of 80 % and a melting point of 180 ^oC. The structure was evaluated using a 1H nuclear magnetic resonance (1H NMR) spectroscopy (Varian Gemini 200 NMR), which was identified as follows:
1H NMR (400 MHz, DMSO) δ 2.92 (s, 6H), 5.92 (s, 1H), 6.79 (d, J = 8.8 Hz, 3H), 7.2 (d, J = 8.4 Hz,

2H), 7.76 (t , J = 7.2 Hz, 1H), 7.85 (t, J = 7.2 Hz, 1H), 7.94 (d, J = 7.2 Hz, 1H), 8.05 (d, J = 7.6 Hz, 1H), 9.09 (s, 1H).

2.2. Electrode preparation and measurement

To use the obtained HBU as an electrode material, different weights percent of VGCF (specific surface area 13 m^2 g^{-1}, fiber length 10–20 lm, aspect ratio 60–70, Showa Denko) (0, 30, 50 and 70) as a conductive additive were mixed with various fractions of HBU (0, 25, 45 and 65) as the active material. 5 wt. % of poly(vinylidene fluoride) (Aldrich) as a polymeric binder with N-methyl-2-pyrrolidinone as a dispersion solvent were mix to form a slurry. The resulting slurry was cast on a platinum as current collector (1.0 cm x 1.0 cm) and then dried at 100 ^{o}C in an oven for 1 hour to vaporize the solvent part. The HBU, VGCF, and the HBU-VGCF powders were probed by means of a Fourier-transform infrared spectroscopy (Bomem MB100). A complex impedance spectroscopy was performed using an Autolab instrument (PGstat 100, Eco Chemie) in the frequency range of 10^2–10^5Hz, with a bias voltage of 0.5 V to compare the conductivity of each sample in aqueous electrolyte of 1M H_2SO_4. In a typical three-electrode electrochemical cell for the cyclic voltammetry measurement, platinum was utilized as the counter electrode, HBU-VGCF as the working electrode, and Ag/AgCl saturated with KCl as reference electrode. 1 M H_2SO_4 was employed as electrolyte in the setup. The cyclic voltammetry was recorded at a potential range -0.2 to 1.4 V vs. Ag/AgCl at various scan rates of 100–1000 mV/s. The specific capacitance (C) as a function of scan rate was calculated using the equation below:

$$C = \frac{|q_a + q_c|}{2m\Delta V} \quad (1)$$

Where ΔV, m and q_a,q_c, represent the voltage window of the cyclic voltammetry, the mass of the active material, and the anodic and cathodic charges on each scan respectively. The surface structures of the prepared electrodes were also perceived using a field emission scanning electron microscope (Hitachi S-4800).

3. RESULTS AND DISCUSSION

The Fourier-transform infrared spectrum in Fig. 2 shows the different blending compositions of the HBU and the VGCF. In the HBU powders, the absorption peak at about 1600 cm^{-1} corresponds to the C=O stretching vibration of quinone groups [50], which is expected to be involved in the 2, 3-dihydro-1,4-naphthoquinone - 1, 4-dihydroxynaphthalene redox pair reactions.

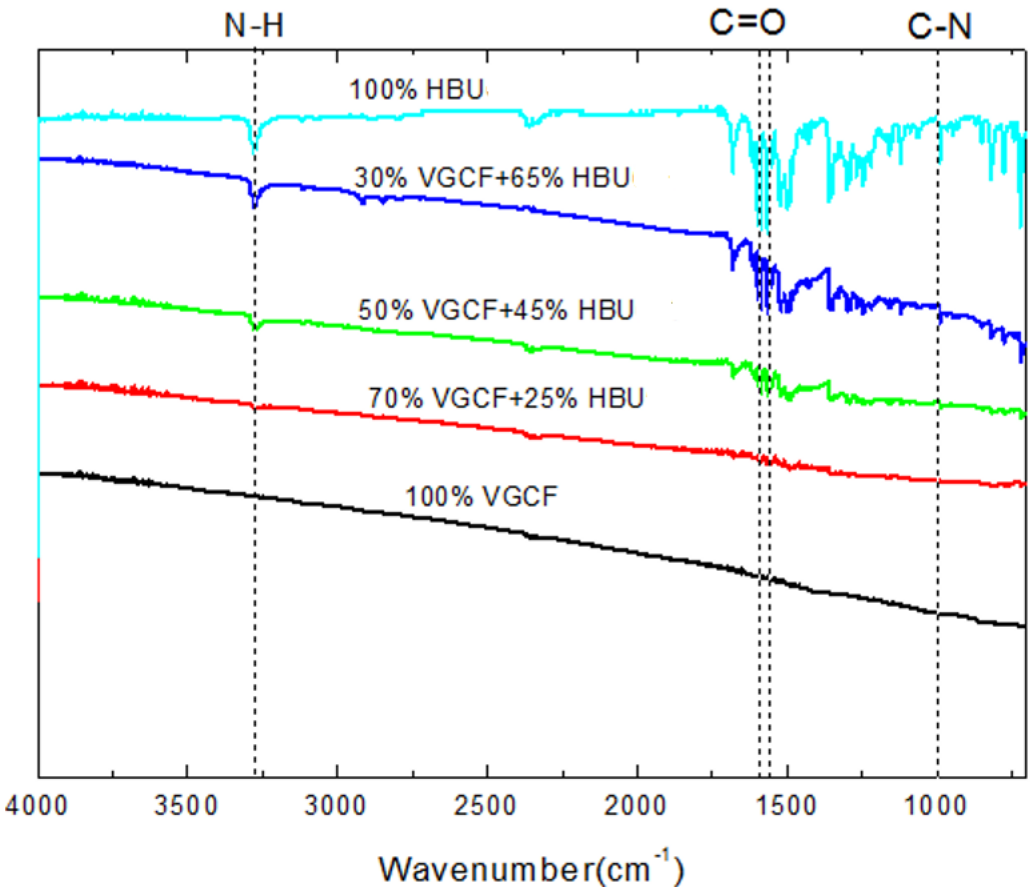

Figure 2. Fourier-transform infrared spectra of the HBU-VGCF with the different weights percent of HBU and VGCF

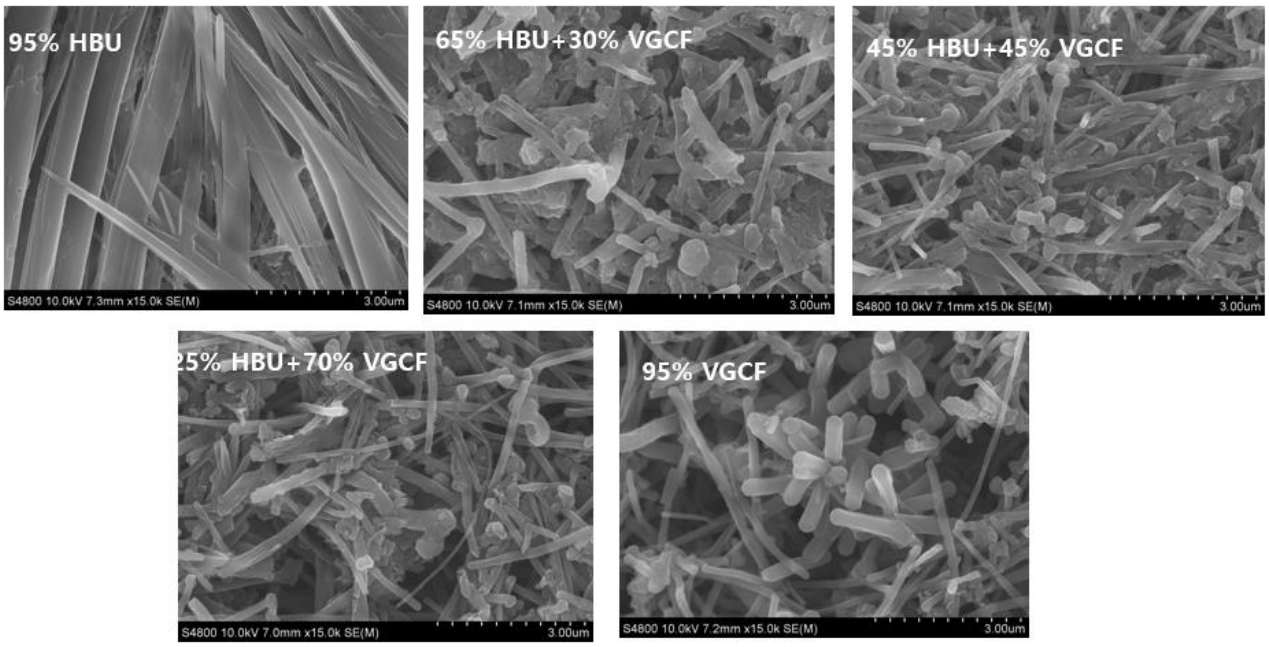

Figure 3. Surface morphologies of the HBU-VGCF with different weight percent of HBU and VGCF

The peak at around 3300 cm^{-1} also appears to correspond to the stretching vibration of the amino

groups (—NH—) in the skeleton of HBU. Again, a stretching corresponding to the C-N (aliphatic amine) wasalso observed in the frame of HBU around 1020 cm^{-1} in the backbone of the substituted derivative of aniline [51]. On the other hand, HBU-VGCF showed minor traces of the —NH— in the skeleton of HBU and the C=O stretching vibration of the quinone group. Nonetheless, VGCF shows no noticeable infrared spectrum band over the whole wave number range.

The surface morphologies of the prepared electrodes are depicted in Fig 3. The VGCF electrode showed a haphazard orientation which accumulates together at certain points. Furthermore, the HBU showed a grass-like or lamella crystalline morphology; however, a change in the morphology of HBU was observed when VGCF was added. In HBU-VGCF with a ratio of 65:30 weight percent, fibrils of VGCF are equally distributed in the HBU, changing its morphology. The addition of VGCF to the HBU also created a porous structure and an effective conducting network, making it possible for VGCF to impact the HBU with the needed electronic conductivity.

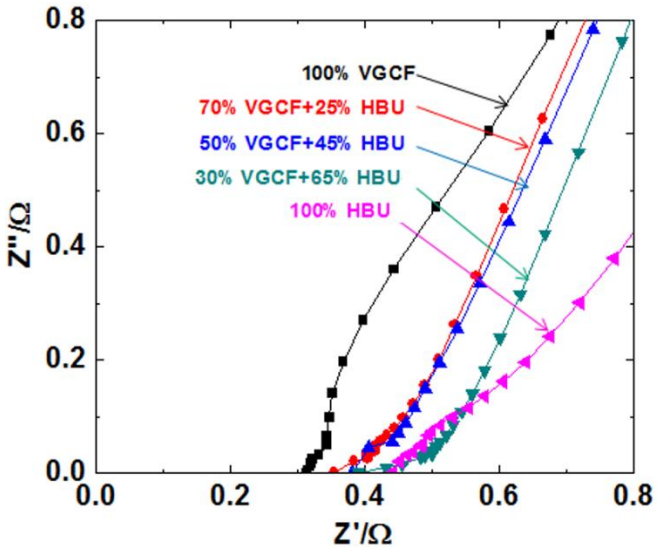

Figure 4. Nyquist plot of the HBU-VGCF with different weights of HBU and VGCF at a bias voltage of 0.5 V

Electrochemical impedance spectroscopy was used to probe the resistive property of the HBU-VGCF electrodes. Comparing the resistive behavior of the prepared electrodes in Fig 4, it can be observed from the intercept on the actual-axis of the Nyquist plot that the VGCF possess lower resistance and hence higher electrical conductivity than the HBU. Incorporating VGCF in the HBU saw an improvement of the interior resistance of the prepared electrodes. Thus the VGCF created a route for the transferal of ions and electrons, thereby decreasing the internal resistance associated with HBU and hence better reversibility.

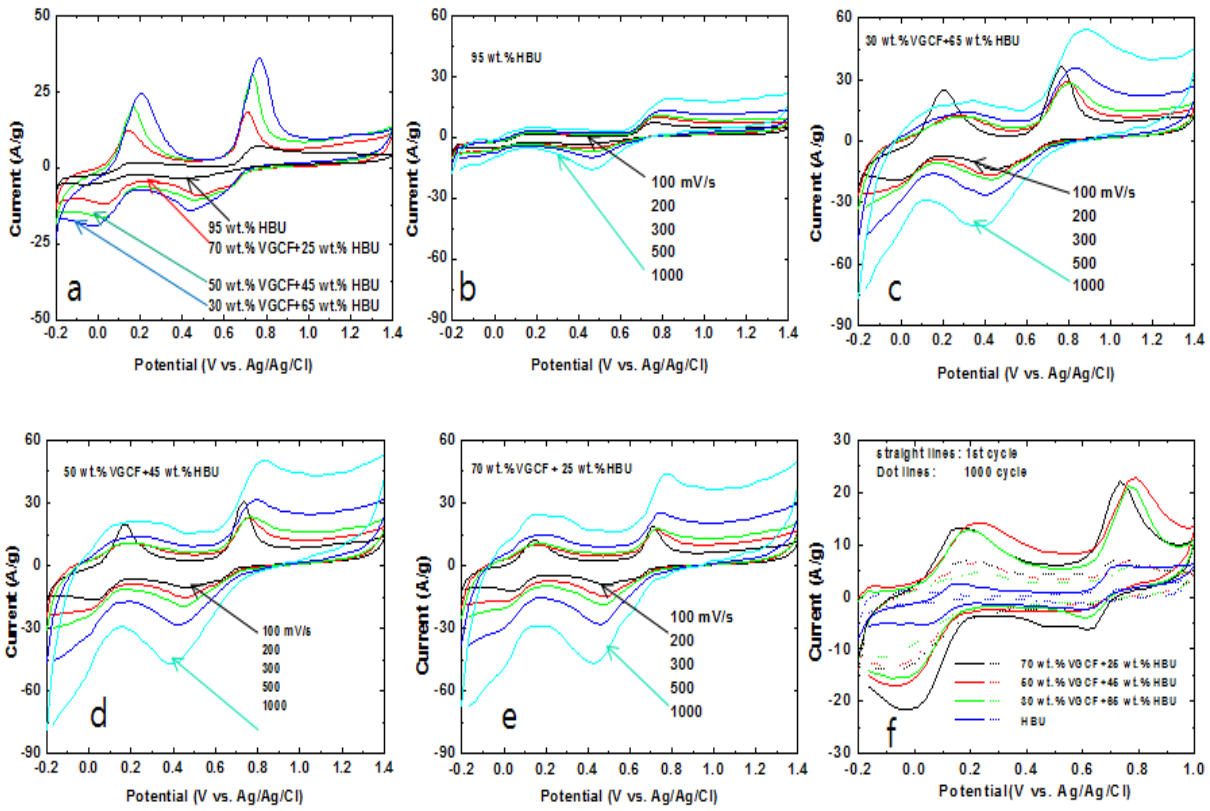

Figure 5. CVs of (a) HBU-VGCF with different weight percent of HBU and VGCF at 100 mV/s (b) 95 wt. % HBU, (c) 30 wt. % VGCF+65 wt. % HBU, (d) 50 wt. % VGCF+45 wt. % HBU and (e) 70 wt. % VGCF+ wt.25% HBU: at different scan rate (f) the 1st and 1000th cycle of HBU-VGCF with different weight percent of HBU and VGCF at -0.2-1.0 V vs. Ag/AgCl and a scan rate of 500 mVs^{-1}

This went a long way to improve the charge storage capability of the HBU and thus, the high capacitance evidenced in the electrodes in Fig 6a. The VGCF serving as a conducting agent assisted the redox reaction involved in the 2, 3-dihydro1,4-naphthoquinone –1,4-dihydroxynaphthalene (PhQ-$PhQH_2$) conversion in the acidic environment ($[H^+] > [Q]$) (see Fig. 1(c)), involving a solo-step $2e^-$, $-2H^+$ redox activity as well as that observed in the redox transition in the aliphatic amine in the HBU structure.

Fig 5a depicts the cyclic voltammograms of the various HBU-VGCF 25:70, 45:50 and 65:30, the pure HBU recorded at 100 mV/s and in a voltage range of 0.2 – 1.4 V. From the CV graphs, the current densities of the HBU-VGCF electrodes were higher compared to the pure HBU. HBU showed a couple of redox peaks at 0.173 V (anodic)/-0.059 V (cathodic), matching a PhQ-$PhQH_2$ redox transition. Again extra peaks matching a redox conversion of the aliphatic amine in the backbone of the substituted derivative of aniline at 0.767 V (anodic)/0.394 V (cathodic) [52] were observed (see fig 1b). Therefore, the redox process of the HBU takes place by a solo-step three-proton ($3H^+$), three-electron ($3e^-$) process. From Fig 4, though the VGCF showed high ionic conductivity due to low resistance, its capacitance contribution is negligible (see Fig 6 a). On the other hand, it is able to make noticeable and reversible the redox processes in HBU. This may be explained as the inherent conductive property of VGCF and the VGCF particles presenting an electronic path way amid the HBU particles. Fig. 5b, 5c, 5e and 5e

show the impact of scan rate on the cyclic voltammetric reaction of the HBU-VGCF electrodes. The impact of iR drop becomes significant in electrodes with fast redox behavior at higher scan rates. The HBU without VGCF showed less pronounced redox peaks of the PhQ-$PhQH_2$ redox activity at higher scan rate; nonetheless, all the HBU-VGCF with the various compositions showed pronounced peaks corresponding to PhQ-$PhQH_2$ as well as those corresponding to the aliphatic amine in the HBU [52]. The porous arrangement of the HBU-VGCF electrodes assisted the solvated ions of the electrolyte to diffuse in and out of the material easily at higher scan rates compared to just the HBU electrode (see SEM data). Furthermore, the shifting of the anodic peak positively and the cathodic peak negatively was reduced, an indication of a reversible system (i.e. making the system less quasi-reversible). The 1st and the 1000th cycles for the HBU-VGCF electrodes in a potential range of -0.2-1.0 V vs. Ag/AgCl and a scan rate of 500 mVs^{-1} is shown in Fig. 5f. As shown in the voltammograms, the redox peaks intensity for all the electrodes reduced with increasing number of cycle, a sign of fading specific capacitance.

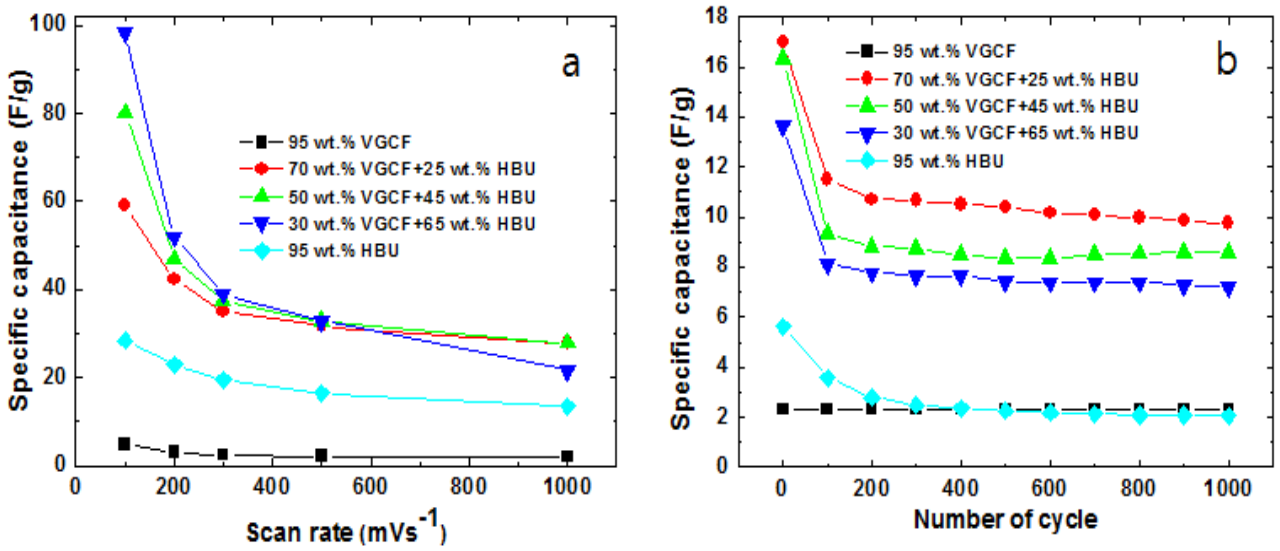

Figure 6. Specific capacitances of HBU-VGCF with different weight percent of HBU and VGCF as functions of (a) scan rate (b) cycle number

A decrease in specific capacitance is observed in all the electrodes with increasing scan rate as shown in Fig. 6a, yet higher capacitance is maintained in all the HBU-VGCF electrodes at higher scan rates compared to just the HBU without VGCF. This capacitance enhancement may be due to the synergistic effect of the VGCF complementing the HBU by creating a better electronic pathway amid the HBU particles and thus boosting the redox transition reaction of PhQ-$PhQH_2$ as well as that of the aliphatic amine in the HBU structure. The cycling stability of specific capacitance is shown in Fig 6b. Capacity retention of about 57 % is observed for the HBU-VGCF electrodes after the 1000th cycle owing to the VGCF supporting the HBU by stabilizing its redox activity. Furthermore, it could be realized from the graph that a higher amount of VGCF is needed to stabilize the HBU.

Table 1. Summary of fiber-based/faradaic pseudocapacitive composite electrode supercapacitors investigated.

Composite electrode	Electrolyte	voltage (V)	Scan rate/current density	Specific capacitance (F/g)	Cell Configuration	Reference
sodium 1,2- naphthoquinone-4-sulfonate doped poly(3,4-ethylenedioxythiophene/ Multi-walled carbon nanotubes	1 M H_2SO_4	-0.5-1.0	5 mV/s	575	3	53
poly (1, 5-diaminoanthraquinone)/ graphene oxide	1 M H_2SO_4	-0.4 - 0.4	1.0 A/g	760	3	54
Polyaniline/ Carbon nanotube	PVA/H_3PO_4	-0.1 – 0.7	5 mV/s	440	3	55
9,10-phenanthrenequinon/ CF500 hybrid-fiber mats	1 M H_2SO_4	-0.4 - 0	10 mV/s	288	3	56
Anthraquinone/ Porous carbon nanotube	1 M H_2SO_4	0 - 0.6	10 mV/s	200	3	57
Pyrrole/ nanocellulose fiber	2.0 M NaCl	0 - 0.8	1 mA cm-2	180	2	58
Carbon nanotube/Nickel Oxide	6 M KOH	0 – 0.55	2 mV/s	713.9	3	59
Polypyrrole/Vapor grown carbon fiber /Acrylonitrile Butadiene Rubber	1 M Na2SO	-0.8 – 0.5	5 mV s-1	125.8	3	60
Carbon nanofiber/Vapor grown carbon fiber/ Polypyrrole	1 M H_2SO_4	0-0.8	1.875 mA/cm^2	678.66	3	61
Cobalt-Nickel Oxide/ vapor grown carbon fiber	1 M KOH	0-0.5	5 mV/s	1271	3	62
Vapor grown carbon fiber/1,4-dihydoxynaphthalene, 2-((4-dimethylamino) phenyl) amino) naphthalene-1,4-dione	1 M H_2SO_4	-0.2-1.4	100 mV/s	98	3	This work

The literature review of carbon fiber-based electrodes for supercapacitors and the findings of the selected investigations are summarized in Table 1. The summary of the various studies outlined the fiber-based/faradaic pseudocapacitive composite electrode used, the working voltage, and the specific capacitance. The fabricated HBU-VGCF electrodes offered specific capacitance of 98 Fg^{-1} at a high rate of 100 mVs^{-1} compared to the most related three-electrode system in the literatures.

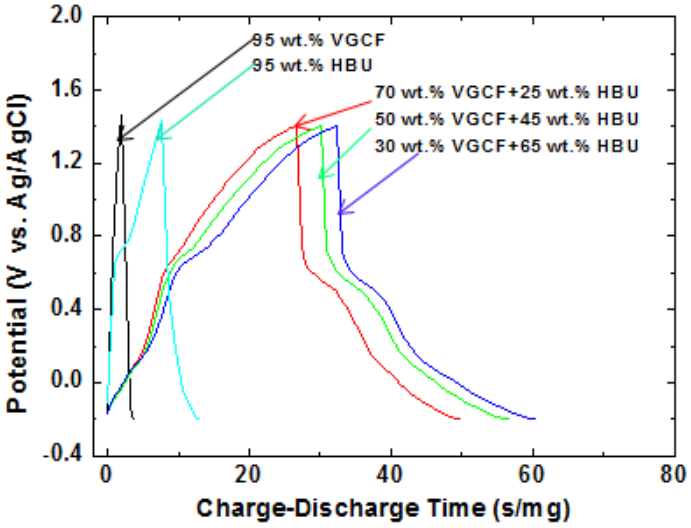

Figure 7. HBU-VGCF with different weight percent of HBU and VGCF, measured at a current density of 5.0 $mAcm^{-2}$

The galvanostatic charge-discharge profile of the HBU-VGCF electrodes are shown in Fig 7 at a 5.0 mA current density and in a voltage range of -0.2-1.4 V vs. Ag/AgCl. All the HBU-VGCF electrodes exhibited an asymmetric charge-discharge profile. The irregularity in the potential curve is the consequence of the redox transitions from the carbonyl groups in the PhQ-$PhQH_2$. Charge-discharge readings were recorded at a constant current; therefore, an extended cycle time signifies that a large amount of electric charges are stored in the supercapacitor and therefore a higher specific capacitance. Maximum charge-discharge time of 62 smg^{-1} is obtained for the HBU-VGCF with the higher weight percent of HBU. Regardless of the short charge-discharge time exhibited by the HBU, an addition of VGCF is able to enhance the charge storage property of the HBU by ensuring effective electron distribution on the surface of the particles.

4. CONCLUSION

The charge storage capacity of a synthesized organic compound, 2-((4-dimethylamino) phenyl) amino) naphthalene-1,4-dione (HBU) was enhanced by the introduction of vapor grown carbon fiber (VGCF). The VGCF created an excellent electronic pathway among the synthesized particles in the electrode, boosting the redox transition reaction in HBU involving a total of three-electron-three-proton processes corresponding to PhQ-$PhQH_2$ and the aliphatic amine in the backbone of the substituted derivative of aniline. This leads to a higher specific capacitance of 98 F/g for the HBU-VGCF electrode with higher weight percent of HBU. Furthermore, the cycling test showed that as the amount of HBU increases, the capacity stability is reduced. Therefore, a balance should be maintained in order to obtain a supercapacitor electrode with good capacity stability as well as high capacitance.

ACKNOWLEDGMENTS
This research was supported by the Basic Science Research Program through the National Research Foundation of Korea (NRF) funded by the Ministry of Education (2013R1A1A2061288).

References

1. J.B. Allen, R.F. Larry, Second edition John Wiley & Sons, Inc, 2001
2. H.P. Wu, D.W. He, Y.S. Wang, M. Fu, Z.L. Liu, J.G. Wang, H.T. Wang, IEEE, (2010) 465-466
3. M.H. Ervina, B.S. Miller, B. Hanrahan, B. Mailly, T. Palacios, Electrochim. Acta, 65 (2012) 37–43.
4. M.A. Pope, S. Korkut, C. Punckt, I.A. Aksay, J. Electrochem. Soc., 160 (2013) A1653–A1660.
5. Y. Wang, Z. Shi, Y. Huang, Y. Ma, C. Wang, M. Chen, Y. Chen, J. Phys. Chem. C, 113 (2009) 13103–13107.
6. L.L. Zhang, X.S. Zhao, Chem. Soc. Rev., 38 (2009) 2520–2531.
7. A.K. Mittal, M.J. Kumar, Encyclopedia Nanosci. Nanotech., 13 (2011) 263–271.
8. Y. Zhang, H. Feng, X. Wu, L. Wang, A. Zhang, T. Xia, H. Dong, X. Li, and L. Zhang, *Int. J. Hydrogen Energy,* 34 (2009) 4889–4899.
9. K. M. Kim, J. H. Nam, Y-G Lee, W. I. Cho, J. M. Ko, *Curr. Appl Phys.,* 13 (2013) 1702-1706
10. E. Frackowiak, F. Béguin, *Carbon*, 39 (2001) 937–950.
11. J.M. Ko, R.Y Song, H.J. Yu, J.W. Yoon, B.G. Min, D.W. Kim, *Electrochim. Acta,* 50 (2004) 873–876.
12. M.Yao, S.Yamazaki, H. Senoh, T. Sakai, T. Kiyobayashi,. *Mat. Sci. Eng. B.,* 177 (2012) 483–487.
13. Y. Hanyu, Y. Ganbe, I. Honma, *J. Power Sources*, 221 (2013) 186–190.
14. W. Wang, W. Xu, L. Cosim bescu, D. Choi, L. Li, Z. Yang, *Chem. Commun*,, 48 (2012) 6669–6671.
15. W. Choi, D.Harada, K. Oyaizu, H. Nishide, *J. Am. Chem. Soc.,* 133 (2011) 19839–19843
16. W. Jung Ha, M. Latifatu, J. Mi, L. H. Soo, K. B. Cheol, H. Louis, P. H. Jeong, K.M. Kwang, K.M Jang, *Synth. Met.*203 (2015) 31–36
17. H. S. Lee, L. Mohammed, B-C. Kim, J. H. Park, Y-G Lee, K. M. Kim, J. Park, Y. G. Baek, J. M. Ko, *Synth. Met.* 217 (2016) 29–36
18. S. Suematsu, K. Naoi, *J. Power Sources,* 97-98 (2001) 816–818
19. J. F. Allen and W. Martin, *Nature*, 445(2007) 610–612.
20. R. E. Blankenship, John Wiley & Sons, Inc, Hoboken, NJ, (2013)
21. M. Cheng, X. Yang, C. Chen, J. Zhao, F. Zhang and L. Sun, *Phys. Chem. Chem. Phys*.,15 (2013) 15146–15152.
22. A. M. Navarro-Suárez, N. Casado, J. Carretero-González, D. Mecerreyes, T. Rojo, *J. Mater. Chem. A***,** 5 (2017) 7137-7143
23. Y. Liang, Y. Jing, S. Gheytani, K.-Y.Lee, P. Liu., A.Facchetti, Y.Yao, *Nat. Mater.,* 16 (2017) 841–848.
24. L. Miao, L. Liu, Y. Li, Y. Lü, F. Cheng, J. Chen, Z.-F. Shang, *Phys. Chem. Chem. Phys*., 20 (2018)13478–13484.
25. D. Walsh, N. M. Sanchez-Ballester, V. P. Ting, K. Ariga and M. T. Weller, *Catal. Sci. Technol.,* 6 (2016) 3718–3722.
26. R. D. Milton, D. P. Hickey, S. Abdellaoui, K. Lim, F. Wu, B. Tan and S. D. Minteer, *Chem. Sci.,* 6(2015) 4867–4875.
27. A. Rodenberg, M. Orazietti, M. Mosberger, C. Bachmann, B. Probst, R. Alberto and P. Hamm, *ChemPhysChem,* 17(2016) 1321–1328
28. Z. Song, H. Zhou, *Energy Environ. Sci.,* 6 (2013) 2280-2301.
29. R. Zeng, L. Xing, Y.Qiu, Y. Wang, W. Huang, W. Li, S. Yang, *Electrochim. Acta,* 146 (2014) 447−454
30. A-L. Barres, J. Geng, G. Bonnard, S. Renault, S. Gottis, O. Mentre, C. Frayret, F. Dolhem, P. Poizot, *Chem. Eur. J*., 18 (2012) 8800−8812
31. M. Yao, H. Senoh, S.-I. Yamazaki, Z. Siroma, T. Sakai, K. Yasuda, *J. Power Sources, 195* (2010) 8336−8340.
32. X. Chen, H. Wang, H. Yi, X. Wang, X. Yan and Z. Guo, *J. Phys. Chem. C,* 118 (2014) 8262–8270
33. H. Wang, F. Li, B. Zhu, L. Guo, Y. Yang, R. Hao, H. Wang, Y. Liu, W. Wang, X. Guo, X. Chen,

Adv. Funct. Mater., 26 (2016) 3472–3479.
34. P. Hu, H. Wang, Y. Yang, J. Yang, J. Lin and L. Guo, *Adv. Mater.,* 28 (2016) 3486–3492.
35. K. Oyaizu, Y. Niibori, A. Takahashi and H. Nishide, *J. Inorg. Organomet. Polym*., 23 (2012) 243–250.
36. D. M. Anjos, J. K. McDonough, E. Perre, G. M. Brown, S. H. Overbury, Y. Gogotsi and V. Presser, Review: *Nano Energy*, 2 (2013) 702–712
37. Z. Huang, Z. Zhang, X. Qi, X. Ren, G. Xu, P. Wan, X. Sun, H. Zhang, *Nanoscale*, 8 (2016) 13273-13279
38. D. Schmidt, M. D. Hager and U. S. Schubert, *Adv. Energy Mater*., 6 (2016) 1500369.
39. S.-K. Kim, Y. K. Kim, H. Lee, S. B. Lee and H. S. Park, *ChemSusChem*, 7 (2014) 1094–1101.
40. M. Zeiger, D. Weingarth and V. Presser, *ChemElectroChem*, 2 (2015) 1117–1127.
41. Y. Zhou, B. Wang, C. Liu, N. Han, X. Xu, F. Zhao, J. Fan and Y. Li, *Nano Energy*, 15 (2015) 654–661.
42. Z. Algharaibeh, X. Liu and P. G. Pickup, *J. Power Sources*, 187 (2009) 640–643.
43. H. W. Cho, L. R. Hepowit, H-S. Nam, S. H. Kim, Y. M. Lee, J. H. Kim, K. M. Kim, J. M. Ko, *Synth. Me.,t* 162 (2012) 410– 413
44. T. Koyama, M. Endo, *Jpn J Appl Phys.,* 3(7) (1974) 1175–6
45. M. Latifatu, H. S. Lee, C. S. Yoon, J. Oh, J. H. Park, J. W. Park, J. M. Ko, *Int. J. Electrochem. Sci*., 11 (2016) 5353 – 5363
46. V. Palomares, A. Goñi, I. G. de Muro, I. de Meatza, M. Bengoechea, I. Canteroc, T. Rojo, *J. Power Sources,* 195 (2010) 7661–7668
47. E. Frackowiak, F. Béguin, *Carbon,* 39 (2001) 937–950.
48. J.S. Speck, M. Endo, M.S. Dresselhaus, *J. Cryst. Growth,* 94 (1989) 834-48
49. G.G. Tibbetts *Appl Phys Lett*., 42 (8) (1983) 666–8
50. S.T. Senthilkumar, R.K. Selvan, N. Ponpandian, J.S. Melo, *RSC Adv*., 2 (2012) 8937–8940
51. J. Yang, H. Dong, *Carbohydr. Polym.,* 153 (2016) 1–6
52. A. Alain, M. C Mohamed, G. Iluminada, P. Jean, and V. Neus, *Langmuir,* 20 (2004) 8243-8253
53. I. S. Vasil'eva, G. P. Shumakovich, M. E. Khlupova, R. B. Vasiliev, V. V. Emets, V. A. Bogdanovskaya, O. V. Morozova and A. I. Yaropolov, , *RSC Adv.,* 10 (2020) 33010
54. N. An, Z. Shao, Z. Guo, J. Xin, Y. He, L. Lv, K. Xie, X. Dong, and Y. Zhang, Z. Hu, *J. power source,* 475 (2020) 228692
55. G. Otrokhov, D. Pankratov, G. Shumakovich, M. Khlupova, Y. Zeifman, I. Vasil'eva, O. Morozova, and A. Yaropolov, *Electrochim. Acta*, 123 (2014) 151–157.
56. M. Zeiger, D. Weingarth, and V. Presser, *ChemElectroChem,* 2 (2015)1117 – 1127
57. S. Chanderpratap, and P. Amit, *J. Phys. Chem. C*, 119 (2015) 11382.
58. Z. Wang, D. O. Carlsson, P. Tammela, K. Hua, P. Zhang, L. Nyholm, and M. Strømme, *ACS Nano,* 9 (7) (2015) 7563–7571
59. Y-H. Lai, S. Gupta, C-H. Hsiao, C-Y. Lee and N-H Tai, *Electrochim. Acta*, (2020) 136744
60. J.-H. Liu, X.-Y. Xu, J. Yu, J.-L. Hong, C. Liu, X. Ouyang, S. Lei, X. Meng, J.-N. Tang, D.-Z. Chen, *Electrochimica Acta*, 314 (2019) 9-19.
61. L. R. Hepowit, K. M. Kim, S. H. Kim, K. S. Ryu, Y. M. Lee, J. M. Ko, *Polym. Bull*., 69 (2012) 873–880
62. Yu Il Yoon, Jang Myoun Ko, *Int. J. Electrochem Sci*., 3 (2008), 1340-1347